

Vascular Section Estimation in Medical Images Using Combined Feature Detection and Evolutionary Optimization

Iván Macía^{1,2} and Manuel Graña²

¹ Vicomtech, Visual Communication Technologies

² Computational Intelligence Group, University of the Basque Country

imacia@vicomtech.org

<http://www.ehu.es/ccwintco>,

<http://www.vicomtech.org>

Abstract. Accurate detection and extraction of 3D vascular structures is a crucial step for many medical image applications that require vascular analysis. Vessel tracking algorithms iteratively follow vascular branches point by point, obtaining geometric descriptors, such as centerlines and sections of branches, that describe patient-specific vasculature. In order to obtain these descriptors, most approaches use specialized scaled vascular feature detectors. However, these detectors may fail due to the presence of nearby spurious structures, incorrect scale or parameter choice or other undesired effects, obtaining incorrect local sections which may lead to unrecoverable errors during the tracking procedure. We propose to combine this approach with an evolutionary optimization framework that use specific modified vascular detectors as cost functions in order to obtain accurate vascular sections when the direct detection approach fails. We demonstrate the validity of this new approach with experiments using real datasets. We also show that, for a family of medialness functions, the procedure can be performed at fixed small scales which is computationally efficient for local kernel-based estimators.

Keywords: Medical Image Analysis, Vascular Analysis, Vessels, Feature Detectors, Evolutionary Optimization, Vascular Tracking, Section Estimator, Medialness, Vesselness.

1 Introduction

Accurate detection and extraction of 3D vascular structures is a crucial step for many medical image applications that require vascular analysis [8][7]. Vascular-related diseases, such as cerebrovascular accidents (stroke) or coronary artery disease, are caused by anomalies in the blood supply, like hemorrhages or blockages. Knowledge of patient-specific vascular structure is crucial for planning many interventions, such as neurointerventions or liver tumor resection. For these applications, many medical imaging modalities exist that are able to depict vessels. Among the most useful ones, we can mention X-ray Angiography,

Computerized Tomography Angiography (CTA) and Magnetic Resonance Angiography (MRA), being the last two 3D modalities.

In order to obtain a meaningful and helpful vascular representation for quantification, visualization or other advanced analysis, it is first necessary to detect and extract the vascular structures with specialized image analysis methods.

Extraction procedures determine which points are part of the vascular structures, by using some measure of *vesselness* (likelihood of being part of a vessel) and geometric and/or appearance models of the vessels [4]. These algorithms usually obtain some geometrical and topological descriptors of the vascular network: the centerline of a vessel is often a good descriptor of the shape of the vessel along its path, and information about the local shape of the vessel is usually obtained by extracting sections along its centerline [8], and if possible by providing estimations of the local radius.

Tracking procedures [4] iteratively find the next vessel (center) point by advancing a given step size (fixed or adaptive) in the direction of the estimated local normal of the current vessel (center) point. However, these local normal and radius (and center point) estimators, which we will call *section estimators*, fail often due to the presence of nearby spurious structures, incorrect scale or parameter selection or other undesired effects. This may result in obtaining incorrect local sections which may lead to unrecoverable errors during the tracking procedure. On the other hand, estimating the correct local section may be interesting in other procedures other than tracking, for example for quantification of the section geometry, local curvature, centerline length, etc.

The present work focuses mainly on improving the accuracy and robustness of the section normal and radius estimation. We propose to combine the standard approach of obtaining a simple solution from the detector response with a non-linear evolutionary optimization procedure. The approach uses a 1+1 evolutionary strategy (ES) algorithm [12] for optimization and a cost function based on the classical section estimator approaches, in order to detect the local optimal orientation and size (radius) of the vascular structure. The optimization may also be useful to find the optimal parameters for the estimators.

The paper is organized as follows: Section 2 is a review of vascular detection and extraction procedures with focus on the methods used on the current work. Section 3 explains the procedure used to combine standard vessel feature detectors with an evolutionary optimization strategy. Section 4 describes some experiments on real datasets and corresponding results with the conclusions summarized on Section 5.

2 Review of Vascular Detection and Extraction

Vascular detection and extraction procedures have been widely reported in the literature. The proposed optimization procedure may be used with a high variety of detectors/estimators, due to its open nature. Here, we will focus on some of the most popular approaches that have been used in our implementation.

The detection procedure usually consists of obtaining a function or metric for every point of an image, called *vesselness function*, that expresses the likelihood of a pixel (voxel) of being part of a vessel structure. The design of such a function is based mainly on the basic property that vessels are usually visible as elongated hyperintense (or hypointense) structures on vascular images. If the vesselness value is higher in the centerline of vessels it is then called *medialness*.

The Hessian matrix is an important tool for vascular detection based on differential operators. For a three dimensional image $I : \mathbb{R}^3 \rightarrow \mathbb{R}$ the Hessian matrix \mathcal{H} is defined as the matrix of (scaled) second order derivatives of the image

$$\mathcal{H}(\mathbf{x}, \sigma) = \begin{bmatrix} I_{xx} & I_{xy} & I_{xz} \\ I_{xy} & I_{yy} & I_{yz} \\ I_{xz} & I_{yz} & I_{zz} \end{bmatrix} \tag{1}$$

which describes the second order local image structure, that is, local image curvatures. The parameter σ is the scaling parameter and corresponds to the Gaussian smoothing, assuming that the derivatives are calculated in scale-space [5].

The three ordered eigenvalues λ_i , $\lambda_1 \leq \lambda_2 \leq \lambda_3$, of this Hessian matrix describe the principal image curvatures which best describe the local image second-order variations. The corresponding eigenvectors v_i describe the directions in which the principal curvatures occur. When the point \mathbf{x} is close to the centerline or medial axis of a vessel and an appropriate scaling parameter is chosen, the local structure of the image is that of a bright (or dark) tubular structure, and the eigenvalues exhibit the following properties [10]:

$$\begin{aligned} \lambda_1 &\approx \lambda_2 \\ \lambda_1, \lambda_2 &\ll 0 \\ \lambda_3 &\approx 0 \end{aligned} \tag{2}$$

This assumes that the local curvature of the vessel is not too high and that the section shows radial symmetry. If these conditions are not met, the eigenvalues differ from this ideal situation.

The eigenvector v_3 corresponds to the direction of the local vessel/tube axis where the curvature barely varies, hence λ_3 is almost zero. The other two principal curvatures, λ_1 and λ_2 , occur in directions that go from the center of the tube to the external part of the vessel, where the curvature varies highly. Hence these eigenvalues are negative and of high absolute value (positive for a dark vessel in a bright background). The associated eigenvectors v_1, v_2 are estimators of the local vessel section plane, since they are aligned with the directions of maximum curvature. Thus, they constitute a *section estimator* as described above.

Several detectors or filters may be designed using these second-order local structure properties. One approach is to take non-linear combination of the eigenvalues, trying to distinguish tube-like local structures from other shapes, such as plate-like or blob-like structures, which exhibit different relationships between the eigenvalues. For example, for plate-like structures two eigenvalues are similar to zero, and blob-like structures show three eigenvalues of the same relatively large value [2]. Of this kind are the methods of Sato *et al.* [10] and

Frangi *et al.* [2] among others. Other approaches estimate the vessel section using the obtained eigenvectors, and then use some sort of differential or integral operator. Examples are the offset medialness measure used by Krissian *et al.* [3] or the ridge detection approach used by Aylward *et al.* [1]. Most of these authors adopt multi-scale approaches, which first select a discrete range of scales, obtain responses for each scale, and then integrate them into a multi-scale representation, usually by taking the maxima across scales. This requires a normalization of derivatives across scales [5]. An estimate of the radius may be obtained by multiplying the scale which gives the maximum vesselness value by a factor which depends on the vessel intensity distribution [3].

The *offset medialness* measure [3] is an integral measure defined in the section plane as:

$$R_{\sigma}^{+}(\mathbf{x}, r) = \frac{1}{2\pi} \int_{\alpha=0}^{2\pi} -\nabla I_{\sigma}(\mathbf{x} + r\mathbf{v}_{\alpha_i}) \cdot \mathbf{v}_{\alpha_i} d\alpha \tag{3}$$

where \mathbf{v}_{α} is a rotating vector, or phasor given by

$$\mathbf{v}_{\alpha} = \mathbf{v}_1 \cos \alpha + \mathbf{v}_2 \sin \alpha \tag{4}$$

Equation 3 is the integral of the projection of the negate of the gradient vector in the radial direction of a circle of radius r around the considered point. This circle is located in the estimated section plane formed by eigenvectors \mathbf{v}_1 and \mathbf{v}_2 . In fact, any other section estimator could be used. As we can see, by tuning r we have an estimate of the local vessel radius.

The corresponding discrete implementation samples the circle points in which the gradient is calculated and corresponds to:

$$R_{\sigma}^{+}(\mathbf{x}, r) = \frac{1}{N} \sum_{i=0}^{N-1} -\nabla I_{\sigma}(\mathbf{x} + r\mathbf{v}_{\alpha_i}) \cdot \mathbf{v}_{\alpha_i}, \quad \alpha = 2\pi i/N \tag{5}$$

Pock *et al.* [9] use the gradient magnitude instead of the gradient projection. We believe that is better to use the projection in the radial direction determined by \mathbf{v}_{α} rather than the gradient magnitude, since spurious or adjacent structures may have a greater undesired contribution in terms of gradient magnitude, which may lead to large values of medialness where it should not. On the other hand, as an improvement, they introduce the following symmetry coefficient:

$$\omega(b_i) = \exp \left[-\frac{1}{2\xi^2} \left(1 - \frac{b_i}{R_{\sigma}^{+}} \right)^2 \right], \quad \xi \in (0, 1] \subset \mathbb{R} \tag{6}$$

where

$$b_i = -\nabla I_{\sigma}(\mathbf{x} + r\mathbf{v}_{\alpha_i}) \cdot \mathbf{v}_{\alpha_i} \tag{7}$$

is the contribution of each radial point, also called *boundariness* [13]. Here, we have used the boundariness measure of Krissian *et al.* [3] but other boundariness measures could be used. The resulting adaptive medialness function is:

$$R_\sigma(\mathbf{x}, r) = \frac{1}{N} \sum_{i=0}^{N-1} \omega(b_i) b_i \quad (8)$$

The symmetry coefficient ξ penalizes asymmetry in the radial distribution of gradient values. When $\xi = 1$ no penalization is performed. The lower the value the more the asymmetry is penalized. There is a trade-off between the asymmetry of the section and the detection rate. If very asymmetrical sections are expected, the value should be one or close to one. Otherwise, $\xi = 0.5$ gives good results in most situations. We also divide the resulting medialness by one plus the gradient magnitude at the center point, since it should be low in a centerline point. This last step was also used by Pock *et al.* [9] but they subtracted this value instead of dividing it.

The original implementation of Krissian *et al.* [3] makes the radius r dependent on the scale in the form $r = \tau\sigma$. In practice, it is not necessary to change r linearly with the scale. Additionally, with large diameters, we would need large scales with increased computational costs. A better approach is to choose a single or a few scales valid enough for the range of diameters to be considered and then adjust r to obtain a maximum response.

Next, we explain our hybrid method of combining this offset medialness measure with an optimization procedure so as to obtain an optimal section estimator.

3 Vascular Feature Detection with Evolutionary Optimization

The vascular feature detection with evolutionary optimization procedure consists of converting a vesselness measure into a cost function that is optimized with respect to a set of parameters. Currently, we use the optimization in order to obtain an optimal section estimator. For this purpose, the vesselness measure needs to be a medialness measure, with the largest values on the vessel axis. In our experiments, we have used the offset medialness measure in eq. 8. The problem can be expressed mathematically as:

$$\arg \max_{\mathbf{u} \in \Omega} R_\sigma(\mathbf{x}_c, \mathbf{u}), \quad \Omega = \{\mathbf{u} = (\mathbf{n}, r) \in \mathbb{R}^4\} \quad \text{s.t.} \quad \|\mathbf{n}\| = 1 \quad (9)$$

The optimization procedure tries to find the optimal unit section normal \mathbf{n} and radius r of the medialness at each section center point \mathbf{x}_c (assuming that is the real vessel section center). This would involve a 4D parameter space for optimization. However, the components of the unit section normal, which are the director cosines, are related to each other by the expression:

$$\|\mathbf{n}\| = \sqrt{n_x^2 + n_y^2 + n_z^2} = 1 \quad (10)$$

Then, the optimization procedure can be expressed as:

$$\arg \max_{\mathbf{u} \in \Omega} R_{\sigma}(\mathbf{x}_c, \mathbf{u}), \quad \Omega = \{\mathbf{u} = (n_x, n_y, r) \in \mathbb{R}^3\} \quad \text{s.t.} \quad \{|n_x| < 1, |n_y| < 1\} \quad (11)$$

This means that we have a 3D search space with two unit normal coordinates and the radius of the detector since the last coordinate is calculated with the above formula¹. The new constraints for the n_x and n_y coordinates can be implemented very easily by returning a zero value for the cost function when the constraints are not met. This is a fast and simple alternative to other more complex approaches such as using Lagrange multipliers.

Note that here the section center is not optimized and it is assumed to be previously calculated, but it could be incorporated into the procedure. The scale σ of the derivative calculations could also be included into the optimization. However, gaussian scale-space derivatives are calculated locally using an implementation with discrete kernels [6] and this would require the calculation of a large kernel at each optimization step.

The procedure for obtaining the section normal then becomes a two stage method (see Figure 1), assuming that we are located on a vessel center point:

1. Estimate the local section using a standard non-optimized estimator. This gives a single solution for the section normal, given the scale, radius and center point. The initial parameters are chosen from the neighbor point if previously calculated. A multiscale approach tests a discrete range of scales and selects the scale that yields the maximum medialness value.
2. Compute the best parameters for the optimization problem in eq. 11 using a (1+1)-ES evolutionary optimizer. Take as starting point the parameters and value of the section normal and radius calculated on the first stage.

Next, we proceed to describe our experiments with real datasets.

4 Experiments and Results

We tested our optimization methods with real 3D datasets, one Contrast-enhanced Magnetic Resonance Image (MRI) of the liver, one Magnetic Resonance Angiography (MRA) of the abdomen and one Computerized Tomography Angiography (CTA) of the abdomen. The resolution of the data was variable, with the liver MRI 1.56x1.56x3.0 mm. spatial resolution, the CTA with 0.72x0.72x1.5 mm. and the MRA 1x1x1.5 mm.

For each dataset, we manually delineated the approximate centerline of one or two long vessels: one major liver vein in the MRI dataset, the aorta in the MRA dataset, and iliac arteries in the other two CTA datasets. The points were interpolated by a B-Spline curve which was then sampled in order to increase the number of centerline points.

¹ Note that this would not be true with standard variable-length vectors.

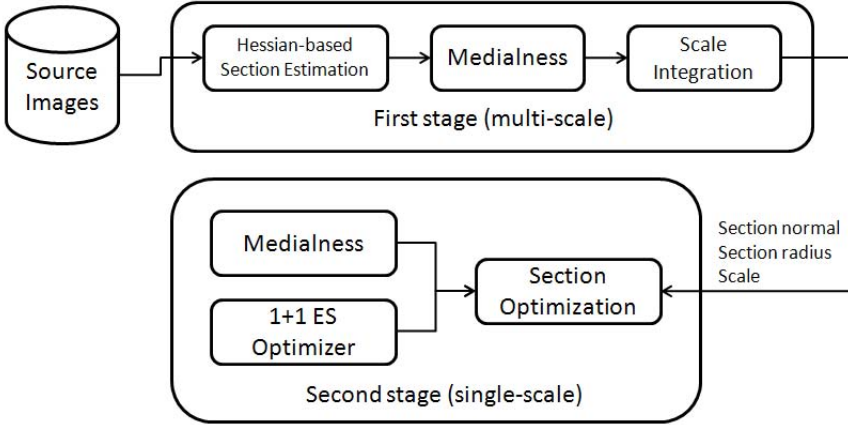


Fig. 1. Two-stage vessel estimation scheme used in our experiments

First, we estimated the sections by the direct method of calculating the eigenvectors of the Hessian matrix. In order to select the scale, for each centerline point, we computed the offset medialness in eq. 8 in the estimated section plane and chose the parameters for the best value (scale, section normal and radius). We used a discrete range of scales ranging from 1.0 to 7.0 using a step size of 1.0. The radius used was the scale times a factor of $\sqrt{3}$ which is a good radius estimate for Gaussian tubes [3]. For all our experiments we used $\xi = 0.5$ for the medialness asymmetry parameter.

Second, we computed the sections with our optimization scheme. In order to keep the two normal components in the range $[-1, 1]$, we simply returned zero as the medialness value outside this interval. The radius was also constrained in the range $[0, R_{max}]$ where R_{max} is chosen above the maximum expected radius value on the images. The scale was fixed in all our experiments to $\sigma = 1.0$, since we found out that the detection was more sensitive to the radius.

The optimization scheme used a non-linear optimization algorithm called (1+1)-Evolution Strategy (ES) [12] as implemented in [14], which belongs to the family of Evolutionary Algorithms [11]. As initial parameters, we chose the normal and the radius from the first step. The medialness was calculated each time on the estimated section. The stop condition was either 5000 iterations or a minimal search radius of 0.25 (Frobenius norm of the covariance matrix). Most of the times the procedure was finished after about 2000 iterations. Note, that our focus here was to test the validity of the approach and not the performance of the optimizer. The latter has quite a lot of margin for improvements, for example, by trying to reduce the search space or by tuning the parameters for optimal performance.

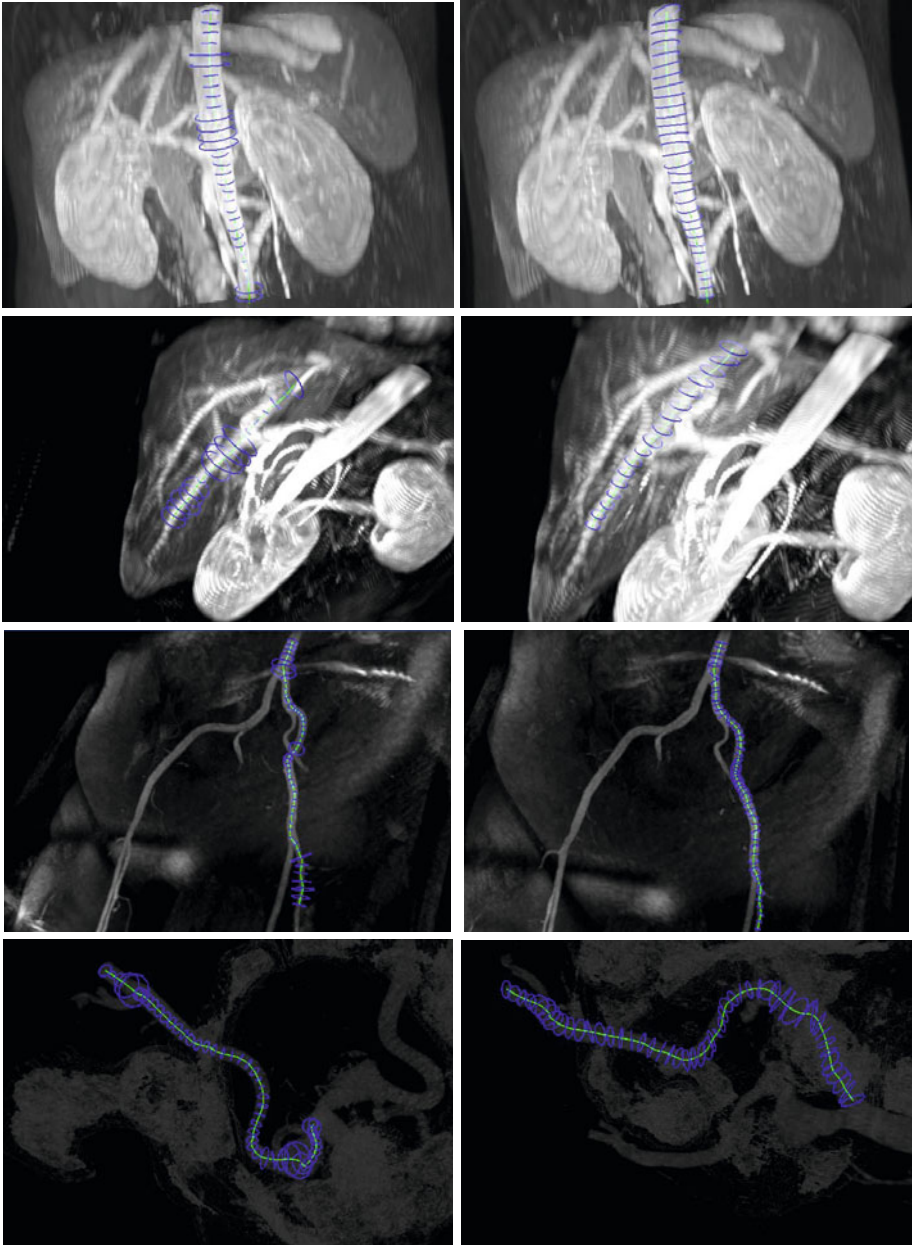


Fig. 2. Volume rendering of real datasets with rendering of estimated vessel sections. Delineated centerlines are shown in green and estimated sections in blue. For each row, from top to bottom, results for an aorta in a MRI, one major liver vessel in the same MRI, and iliac arteries for a MRA (third row) and CTA (fourth row) study. Left column depicts the results of the first, direction estimation stage. Right column shows the results after the evolutionary optimization procedure.

Results of the described method for both stages are shown in Fig. 2. The 3D render shows the estimated sections and radius depicted as circles at each centerline point (actually we did not draw all the centerline points but only a subset). Note that the standard estimator works quite well at estimating the sections. This is normal since most of the vessels were clearly visible. However, there was a high variation in the scale and radius estimation along the vessels. The optimized procedure shows very precise results at estimating the section and radius, except maybe at bifurcations, where the first stage also fails. Note specially that the accuracy in the radius estimation is really high, which would be difficult to estimate by manually setting the parameter on the first stage.

It is important to highlight the fact that our method can be applied to virtually any vesselness function. In this sense, the method can be thought of as both a shape and parameter estimator, thus decreasing the number of parameters of the original estimator. In our experiments, we have initialized the parameters for each section independently of the results of the previous optimization. However, the optimizer can be initialized with an initial position corresponding to the previously calculated point. In this way, the optimization procedure would be less time consuming.

The optimization stage is slower than the previous step (in the order of minutes, rather than in the order of seconds). In practice, it should only be used when we accurate values of radius and section normal are required or when the value of the direct section estimator is likely to be incorrect. During a tracking procedure, this can be detected as an outlier, for example, when the normal exceeds an angle with respect the previous normal along the vessel path (assuming that the step size is small enough). It may also be used as a parameter estimator for the standard procedure obtaining parameter values to be used in a given application.

On the other hand, the scale for the medialness was fixed to a small value in the optimization stage. The reason is that the scale for this family of medialness function should be chosen according to the size of the vessel boundaries (the boundary is relatively thin) and not according to the diameter. Otherwise, precision would also be penalized, since we would have a poorer localization with higher scales. This is an important conclusion, since we have observed that, for these types of vesselness functions, we can operate at lower scales and with less variability. The reason is that the scale of the diameters may vary considerably but the scale of the vessel boundaries not so much. For local calculations using discrete kernels, this supposes smaller kernels and less kernel recalculations, which is computationally faster. The procedure also does not require estimating the Hessian at each iteration, which makes it faster than expected.

5 Conclusions and Future Work

We have developed a method for the estimation of vessel sections on medical images. It uses an evolutionary optimization scheme together with well-known vascular feature detectors. These were adapted as cost functions and acted as

section estimators for the section normal and radius. This alternative approach is used after a standard direct multiscale section estimator stage. In the current work, we have used a family of medialness functions as section estimators, although the method admits other types of estimators. We have tested the validity of the approach by estimating the vessel sections of delineated vessel centerlines on real MRI, MRA and CTA datasets. Our results show improved accuracy, more evident in the radius estimation, at the expense of extra computational time. The procedure can be used as a high accuracy estimator, as a backup stage during a tracking procedure or as a parameter estimation for several vessel feature detectors.

Future work will be focused on more exhaustive experimental work, extending the approach to use other types of section estimators and improving the performance of the optimization procedure.

References

1. Aylward, S.R., Bullitt, E.: Initialization, noise, singularities, and scale in height ridge traversal for tubular object centerline extraction. *IEEE Trans. Med. Imaging* 21(2), 61–75 (2002)
2. Frangi, A.F., Niessen, W.J., Vincken, K.L., Viergever, M.A.: Multiscale Vessel Enhancement Filtering. In: Wells, W.M., Colchester, A.C.F., Delp, S.L. (eds.) *MICCAI 1998*. LNCS, vol. 1496, pp. 130–137. Springer, Heidelberg (1998)
3. Krissian, K., Malandain, G., Ayache, N., Vaillant, R., Troussset, Y.: Model based detection of tubular structures in 3d images. *Computer Vision and Image Understanding* 80(2), 130–171 (2000)
4. Lesage, D., Angelini, E., Bloch, I., Funka-Lea, G.: A review of 3d vessel lumen segmentation techniques: Models, features and extraction schemes. *Medical Image Analysis* 13(6), 819–845 (2009)
5. Lindeberg, T.: Discrete derivative approximations with scale-space properties: A basis for low-level feature extraction. *J. Math. Imaging Vision* 3, 349–376 (1993)
6. Macía, I.: Generalized computation of gaussian derivatives using itk. *The Insight Journal* (December 2007)
7. Macía, I., Graña, M., Maiora, J., Paloc, C., de Blas, M.: Detection of type ii endoleaks in abdominal aortic aneurysms after endovascular repair. *Computers in Medicine and Biology* 41(10), 871–889 (2011)
8. Macía, I., Graña, M., Paloc, C.: Knowledge management in image-based analysis of blood vessel structures. *Knowledge and Information Systems* 30(2), 457–491 (2012)
9. Pock, T., Janko, C., Beichel, R., Bischof, H.: Multiscale medialness for robust segmentation of 3d tubular structures. In: *10th Computer Vision Winter Workshop* (2005)
10. Sato, Y., Nakajima, S., Shiraga, N., Atsumi, H., Yoshida, S., Koller, T., Gerig, G., Kikinis, R.: 3d multi-scale line filter for segmentation and visualization of curvilinear structures in medical images. *Medical Image Analysis* 2(2), 143–168 (1998)

11. Schwefel, H.P.: Evolution and Optimum Seeking. Wiley (1995)
12. Styner, M., Brechbuhler, C., Székely, G., Gerig, G.: Parametric estimate of intensity inhomogeneities applied to mri. *Trans. Med. Imag* 19(3), 153–165 (2000)
13. Xu, M., Pycock, D.: A scale-space medialness transform based on boundary concordance voting. *J. of Math. Imag. and Vision* 11(3), 277–299 (1999)
14. Yoo, T.S., Ackerman, M., Lorensen, W., Schroeder, W., Chalana, V., Aylward, S., Metaxas, D., Whitaker, R.: Engineering and algorithm design for an image processing api: a technical report on itk - the insight toolkit. *Stud. Health. Technol. Inform.* 85, 586–592 (2002)